

Study of coupling loss on bi-columnar BSCCO/Ag tapes by a.c. susceptibility measurements

D. Zola,* M. Polichetti, and S. Pace

*Department of Physics “E. R. Caianiello”, and INFM Research Unit,
University of Salerno, via S. Allende, I-84081 Baronissi, (Salerno), Italy.*

F. Gömöry, F. Strýček, E. Seiler, I. Hušek, and P. Kováč

*Institute of Electrical Engineering, Slovak Academy of Sciences,
Dubravska Cesta 9 842 39 Bratislava, Slovakia*

(Dated: November 4, 2018)

Coupling losses were studied in composite tapes containing superconducting material in the form of two separate stacks of densely packed filaments embedded in a metallic matrix of Ag or Ag alloy. This kind of sample geometry is quite favorable for studying the coupling currents and in particular the role of superconducting bridges between filaments. By using a.c. susceptibility technique, the electromagnetic losses as function of a.c. magnetic field amplitude and frequency were measured at the temperature $T = 77$ K for two tapes with different matrix composition. The length of samples was varied by subsequent cutting in order to investigate its influence on the dynamics of magnetic flux penetration. The geometrical factor χ_0 which takes into account the demagnetizing effects was established from a.c. susceptibility data at low amplitudes. Losses vs frequency dependencies have been found to agree nicely with the theoretical model developed for round multifilamentary wires. Applying this model, the effective resistivity of the matrix was determined for each tape, by using only measured quantities. For the tape with pure silver matrix its value was found to be larger than what predicted by the theory for given metal resistivity and filamentary architecture. On the contrary, in the sample with a Ag/Mg alloy matrix, an effective resistivity much lower than expected was determined. We explain these discrepancies by taking into account the properties of the electrical contact of the interface between the superconducting filaments and the normal matrix. In the case of soft matrix of pure Ag, this is of poor quality, while the properties of alloy matrix seem to provoke an extensive creation of intergrowths which can be actually observed in this kind of samples.

PACS numbers: 74.81.Bd; 74.25.Ha; 84.71.Mn

Keywords: a.c. losses, BSCCO(2223)/Ag tapes, a.c. susceptibility

I. INTRODUCTION

BSCCO/Ag tapes usually contain many superconducting filaments embedded in a silver or silver alloy matrix. For achieving thermal stability and quench protection, the metallic matrix with high thermal conductivity should have a good interface with the superconducting material. When the tape is immersed in alternating (a.c.) magnetic field, an energy loss is observed that is caused by various mechanisms^{1,2}. The irreversible magnetisation is an intrinsic property of type II superconductors, and the energy loss related to it is usually called “hysteretic loss”. The a.c. magnetic field induces also an electrical field which drives currents in the loops formed by pairs of filaments and closed by crossing the metallic matrix. The ohmic loss generated in the metallic part of the loop is accordingly called “coupling loss”. Finally, the currents, which flow in metallic matrix only, give rise to the so called “eddy currents loss”. The latter contribution can be often omitted at the power grid frequency. In general, it is desirable to take measures that reduce the different kinds of losses. To reduce the hysteretic losses, the dimensions of superconducting filaments have to be diminished. To cut down the coupling losses, it is essential to reduce the area of induced flux

e.g. by twisting the filaments. Moreover, the matrix resistivity should rise, for example by manufacturing an artificial resistive barrier around the filaments. The effective resistivity of the paths that the coupling currents follow generally differs from the bare matrix resistivity, because it depends on the tape geometry and on the particular arrangement of the superconducting filaments. It is often used to characterize the coupling currents by the time constant τ of magnetic flux penetration. As shown by Kwasnitza³, the coupling loss can be expressed as a function of $\omega\tau$ ($\omega = 2\pi\nu$) at constant a.c. magnetic field amplitude (B_0). In other words, the coupling loss is well characterized by this time constant. For example, in an application working at frequency ν the tape should be used that exhibits the time constant such that $2\pi\nu\tau \ll 1$ to avoid the saturation of the filaments just by the induced coupling currents. Existing theories provide formulas for the time constant in a tape with known geometry and matrix resistivity. Unfortunately, in HTS tapes the experimental data on the time constant can be very different from the calculated value because of the irregularities in the interface between the filaments and the matrix. Therefore it is necessary to understand how the coupling loss works in real BSCCO/Ag tapes. Moreover it is necessary to understand what is the metallic matrix

which has the best effective resistivity.

Thorough investigations have been carried out on coupling loss in HTS tapes^{4,5,6,7,8,9,10}. However, it is still not evident whether the coupling mechanism in BSCCO/Ag can be analyzed in the same manner as for low T_c wires. In this paper, this kind of losses has been studied in tapes with a geometry resembling just two filaments separated by a metallic matrix. In reality, each "filament" consists in dense stack of extremely flat filaments. In this way a simple geometry has been achieved, allowing us to study the coupling currents without other spurious effects. We have measured the time constant and determined the effective resistivity for two such bi-columnar tapes that differ significantly in the matrix composition and thus in its resistivity. The external magnetic field (B_a) was always perpendicular to the broad face of the sample. The geometrical factor χ_0 (related to demagnetizing factor)^{11,12} has been measured. In order to study the effect of the sample length on the losses, the measurements were repeated for the same tape, cut several times in always shorter pieces. In this way we could discuss the various aspects of coupling losses in this system and make a comparison with the most used model¹³ in this field. The importance of the intergrowths between the superconducting filaments on the coupling losses is also pointed out.

II. THEORETICAL BACKGROUND

The coupling loss per unit volume and per cycle (Q_c) depends mainly on $\omega\tau$ and on the square of the a.c. field amplitude (B_0). Several authors give expressions of Q_c for harmonic external fields, perpendicular to the broad face of the tape^{3,4,13,14}. In our analysis the Campbell model has been used¹³. The model assumes that the superconductor is divided into many filaments and the magnetic field (B) inside the composite conductor, averaged on many filaments, is uniform. From this last requirement it follows that the coupling currents flow in the outer shell of the wire¹³. Since these currents are proportional to the time derivative (\dot{B}) of internal magnetic field B , we can write the relation

$$B = B_a - \tau \dot{B} \quad (1)$$

where B_a is the applied magnetic field. The proportionality constant τ is called *time constant* of the tape and the theory states that it is related to the sample geometry (the cross section as well as the length) and to the matrix resistivity. τ is also the time decay of the coupling currents if the external magnetic field B_a becomes instantaneously constant. For this reason, in principle, the time constant could be measured by magnetic relaxation measurements. Nevertheless these measurements are influenced by the relaxation of the irreversible magnetisation of the superconducting filaments and by the overshoot of the magnetic field produced by the magnet¹⁵. By integrating the Eq. (1) it is possible to calculate the coupling

loss density (Q_c) for a sinusoidal external field:

$$Q_c = \frac{B_0^2}{2\mu_0} \left[2\pi\chi_0 \left(\frac{\omega\tau}{1 + \omega^2\tau^2} \right) \right] \quad (2)$$

where χ_0 is the demagnetization factor in the actual sample vs. field geometry. The expression in square brackets is independent of magnetic field amplitude. Moreover we can suppose that the frequency dependence predicted by eq. (2) is still valid also in presence of few filaments. In this case we can expect that the eq. (2) has to be corrected by a numerical factor:

$$Q'_c = \gamma Q_c \quad (3)$$

On the other hand the a.c. losses are related to the imaginary part of the first harmonic of the a.c. susceptibility^{2,11} and can be expressed as:

$$Q = \pi\chi''\chi_0 B_0^2/\mu_0 \quad (4)$$

where χ'' is the imaginary part of the a.c. susceptibility. By supposing that the losses are dominated by coupling mechanism it holds:

$$\chi'' = \gamma \frac{\omega\tau}{1 + \omega^2\tau^2} \quad (5)$$

By measuring the loss as a function of frequency (ν) at fixed B_0 , the time constant can be determined by finding the frequency (ν_m) where the maximum occurs, corresponding to $\omega\tau = 1$. On the other hand, in the low frequency limit Q_c depends linearly on τ and therefore, τ can be evaluated by measuring magnetisation loops for different sweep rates of a small external field¹⁶. Nevertheless the linear dependence has to be separated from the logarithmic dependence due to the flux creep in the filaments¹⁷, which has not been considered in the Campbell model.

The equation (2) is no more valid when the filaments become saturated by currents, i.e. the current density is equal to the critical current density in the whole section of the filament. In fact for B_0 values larger than the full penetration field of a single superconducting filament (B_{pf}), or as ωB_0 becomes quite large, the currents saturate the outer filaments. Then the filaments behave as fully coupled and the coupling loss turns to be hysteretic. Since the coupling currents propagate inside the specimen, the field inside the sample is no more uniform, which was the key assumption for the validity of the equation (2). On the other hand, for increasing B_0 , the magnetic moment of the sample rises. Nevertheless, it cannot exceed the magnetic moment of an equivalent superconducting tape with a single core offering the identical cross section and the same J_c of the multifilamentary tape. Therefore at high field, the losses of a multifilamentary tape can be found from the area of the hysteresis loop of the equivalent monocoil tape. This upper limit of loss can be exactly evaluated by taking into account the sample geometry. Nevertheless, for $B_0 \gg B_{ps}$ (where B_{ps} is

the magnetic field where the saturation in the magnetisation occurs) one can neglect the actual shape of $M(B_a)$ loop and the extremities of $M(B_a)$ loops can be approximate by upright straight lines. Thus, the saturation loss is written as:

$$Q_c = 4\mu_0 M_s B_0 \quad (6)$$

where M_s is the saturation magnetisation.

As far as the frequency dependence is concerned, for $B_0 \gg B_{ps}$, as the frequency increases, the losses saturate at a constant value¹³ given by eq. (6) which is, in a first approximation, frequency independent. Also in this case, going more insight, Q_c should be considered as frequency dependent due to the frequency dependence of M_s which is not always negligible in high T_c superconductors¹⁷.

A. Expressions for time constant

Theoretical expressions for τ can be found by calculating the electrical field E inside the tape and the power loss density $p = E^2/\rho_m$, where ρ_m is the effective resistivity of the metallic matrix. At low frequencies this quantity can be compared to the expression given by the Campbell model¹³:

$$p = \chi_0 \tau \frac{\dot{B}^2}{2\mu_0} \quad (7)$$

to extract τ . In literature, expressions for τ are reported⁹, for twisted and untwisted flat cable, for external magnetic field either perpendicular or parallel to the broad face of the tape. In our case, the samples are untwisted BSCCO tapes and the expression for τ is:

$$\tau = \frac{\ell^2 \mu_0}{\pi^2 \chi_0 \rho_m} \quad (8)$$

showing that the time constant depends on the square of the length, on the resistivity and on the tape geometry (represented by χ_0 factor).

If χ_0 is 1 (the value for a slab geometry) the previous expression is identical to the expression for τ found solving the flux diffusion equation in a slab.

B. Effective resistivity

In the expression (8), the effective resistivity depends also on the arrangement of the filaments in the tape. Carr¹⁸ has shown that, in the continuum anisotropic model, the effective resistivity is defined in terms of the matrix resistivity ρ_m and the superconducting volume fraction η_{eff} related to the elementary zone alone. In BSCCO tape η_{eff} is larger than the superconducting fraction η due to a presence of an external metallic sheath that embeds the filaments. In the particular case of a

round wire, and supposing that the electrical contact between the metallic matrix and the superconducting filaments is good, the effective resistivity is lower than ρ_m and it is given by¹⁸:

$$\rho_{eff} = \rho_m \frac{1 - \eta_{eff}}{1 + \eta_{eff}} \quad (9)$$

If the electrical contact is bad, giving a high resistive barrier around each filament, ρ_{eff} increases in comparison with the resistivity of the matrix, according to the expression¹⁸:

$$\rho_{eff} = \rho_m \frac{1 + \eta_{eff}}{1 - \eta_{eff}} \quad (10)$$

In our sample, there was no artificially involved resistive barrier. We also assume that heat treatments commonly increases the quality of the electrical contact between filaments and matrix. Modification of the expressions (9) and (10), taking into account geometries more similar to our samples, have been calculated¹⁹, yielding for the geometry of our samples the ratio ρ_{eff}/ρ_m as:

$$\frac{\rho_{eff}}{\rho_m} = \frac{t_u w_u - t_u w_f}{t_u w_u - t_u w_f + t_f w_f} \quad (11)$$

where the meaning of t_u , t_f , w_u , and w_c is shown in Fig. 1. Introducing the effective superconducting fraction $\eta_{eff} = (w_f t_f)/(w_u t_u)$, the last equation can be written as:

$$\frac{\rho_{eff}}{\rho_m} = \frac{1 - \frac{w_f}{w_u}}{1 - \frac{w_f}{w_u} + \eta_{eff}} \quad (12)$$

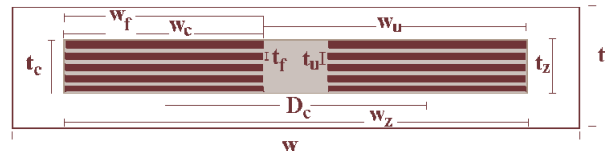


FIG. 1: Schematic cross section of the tape. w and t are respectively the width and the thickness of the tape. w_z and t_z are the dimensions of the elementary zone. w_c and t_c are respectively the width and the thickness of the two columns. t_f is the filament thickness, whereas w_f is the filament width. w_u is the column width plus the distance between the two columns, whereas t_u is the filament thickness plus the distance between the neighbor filaments. Finally D_c is the distance between the columns centers.

C. Theoretical values of χ_0

For a superconductor in Meissner state, the χ_0 expressions for infinite strip and finite x-z array have been reported by Fabbriatore et al.^{11,12}.

If our samples are considered like a single strip with rectangular cross section, χ_0 is given by:

$$\chi_0 = \frac{\pi w_z}{4d_z} \quad (13)$$

where w_z and d_z are respectively the width and the thickness of the filamentary zone. For a more realistic geometry like a finite x-z array with 2×8 filaments, the expression for χ_0 is very complicate and is given by:

$$\chi_0 = \chi_0(1) \frac{f_x}{f_z} \quad (14)$$

where $\chi_0(1) = \pi w_f / 4t_f$, is the geometrical factor calculated according to Eq. (13), and

$$f_x = \left[1 + \frac{2}{\pi} (\beta - 1) \operatorname{arcsec} \left(\frac{n_x + 5\beta - 1}{5\beta} \right) \right]; \quad (15)$$

$$f_z = \chi_0(1) \left(\chi_0(z - \infty) + \frac{\chi_0(1) - \chi_0(z - \infty)}{n_z^{0.8}} \right)^{-1}; \quad (16)$$

where n_x is the number of filaments in the x direction and n_z is the number of filaments in z direction. Moreover

$$\beta = \frac{\chi_0(x - \infty) D_c d_f + D_c - w_f}{\chi_0(1) w_f D_c - w_f} \quad (17)$$

where²⁰

$$\chi_0(x - \infty) = -\frac{2D_c^2}{\pi w_f t_f} \ln \left[\cos \left(\frac{\pi w_f}{2D_c} \right) \right]; \quad (18)$$

$$\chi_0(z - \infty) = \frac{2t_u^2}{\pi w_f t_f} \ln \left[\cosh \left(\frac{\pi w_f}{2t_u} \right) \right]; \quad (19)$$

and D_c is the distance between the centers of each column, whereas t_u is the distance between the centers of two neighbor filaments.

III. EXPERIMENTAL DETAILS

A. The samples

The behaviour of two different kinds of bi-columnar BSCCO(2223) tapes has been investigated by means of the a.c. susceptibility technique. The first BSCCO/Ag tape (named sample **A**) was prepared with 16 filaments in pure silver matrix with a stack of 8 filaments for each column separated by about 0.3 mm of pure silver. The external sheath is also made with the same material. The geometry of the second sample (sample **B**) is very similar to that of the sample **A**, but the number of filaments is 15 and therefore there are 8 filaments in one column and 7 in the other. The metallic sheet between filaments is a Ag/Mg(0.4%) alloy and the matrix which embeds the whole filamentary zone is a

Ag/Mg(0.4%)/Ni(0.22%) alloy. For both samples, strong bridging could be present between filaments in the same column. The initial length of the sample **A** was 61.7 mm, whereas the sample **B** was 61.6 mm long. Preliminary transport measurements have shown that sample **A** has a higher critical current than sample **B**. This indicates that the grains alignment or the grains connectivity in sample **B** is worse than in sample **A**. The main features of the samples are summarized in Tab. I and in Fig. 2 the cross section of the sample **A** is shown. In Tab. II the different sizes are reported.

Sample	A	B
matrix	Ag	Ag/Mg(0.4%)
External sheath	Ag	Ag/Mg(0.4%)Ni(0.22%)
fill factor (η)	32 %	32%
width (w)	3.3 mm	3.1 mm
thickness (t)	0.25 mm	0.24 mm
initial length (ℓ)	61.7 mm	61.6 mm
critical current (I_c)	23.5 A	17.5 A
c. c. density (J_c)	9653 A/cm ²	7173 A/cm ²
exponent (n)	15	15

TABLE I: Main features of the samples **A** and **B**



FIG. 2: Cross section of BSCCO/Ag sample **A**

In the samples **A** and **B**, the resistivity of the different matrices was experimentally measured by a D.C. transport measurement on samples without superconducting material. For pure Ag matrix $\rho_m = 0.27 \mu\Omega \text{ cm}$, while the resistivity of the Ag/Mg alloy is $\rho_m = 1.08 \mu\Omega \text{ cm}$. By using the expression (8) and the dimensions reported in Tab. II, the expected ratio ρ_{eff}/ρ_m is 0.25. Therefore the expected effective resistivity for the Sample **A** is $0.068 \mu\Omega \text{ cm}$, while it is $0.27 \mu\Omega \text{ cm}$ for the sample **B**. Finally, the estimated value for η_{eff} is 71%.

w_c (mm)	t_c (mm)	D_c (mm)	w_z (mm)	t_z (mm)
1.0	0.21	1.3	2.3	0.21
w_u (mm)	t_u (mm)	w_f (mm)	t_f (mm)	$t_u - t_f$ (mm)
1.3	0.027	1.0	$\simeq 0.025$	$\simeq 0.002$

TABLE II: Geometrical dimensions of the tapes as defined in Fig. 1

B. A.C. loss measurements

The a.c. losses were measured by using the standard a.c. susceptibility technique. An a.c. susceptometer with

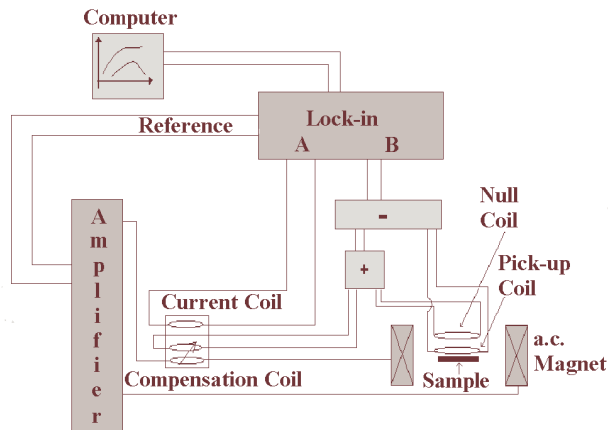


FIG. 3: Sketch of the experimental set-up employed for a.c. measurements

a system of coils suitable for measurements on sample with length up to 12 cm is sketched in Fig. 3. The susceptometer comprises a.c. electromagnet which produces an a.c. magnetic field with B_0 up to 50 mT, with a field homogeneity within 1% on a 8 cm length and 2% on 12 cm. The power to the a.c. magnet is delivered by an amplifier controlled by the signal from the internal oscillator of the lock-in amplifier. The a.c. field induces a voltage in two coils: the pick-up coil, which is very close to the sample surface, while the second, the null coil, which is 1 cm apart. The a.c. magnet and both the coils are placed in a reinforced plastic cryostat, so no eddy currents are induced in the cryostat walls. The system is cooled by liquid nitrogen and all the measurements have been performed at 77 K. Since the pick-up coil and the null coil are not perfectly identical, a variable compensation system is also used. The input signal for the lock-in is the result of the difference between the pick-up voltage and the sum of the null and the compensation voltages. The current which flows in the a.c. magnet is inductively measured by the current coil.

The two original full length samples were subsequently cut several times to vary the sample lengths. In each of these operations, the tape boundaries were polished and protected with grease. Measurements were performed in the frequency range from 1 Hz to 1000 Hz in the field amplitude ranging from 0.05 mT to 45 mT.

C. Experimental measurement of χ_0

To experimentally evaluate the χ_0 value of the samples, the technique described in detail by Fabbriatore et al.¹²

was used. By performing the measurement at very low magnetic field amplitude (such as to assure the Meissner state), the constant χ_0 can be determined by using the relation:

$$\chi_0 = G_c \frac{V_{coil}}{V_{sample}} \frac{U_{meas}}{U_{coil}} \quad (20)$$

where U_{meas} is the in input signal of the lock-in amplifier when the sample is placed in the pick-up coil, U_{coil} is the voltage of null coil only, V_{sample} is the volume of superconducting fraction, V_{coil} is the volume of the pick-up coil and G_c is a constant depending on the geometry of the coils.

IV. EXPERIMENTAL RESULTS

A. Determination of χ_0

The value of χ_0 was measured on a samples of 6.4 mm length at the frequencies of 7 Hz and 21 Hz.

In order to check the frequency dependence of χ_0 , measurements in the frequency range between 7 Hz and 710 Hz, reported in Fig. 4, were performed on the sample **A**. All these measurements were done at the magnetic field amplitude of 1.3 G, enough to achieve a complete shielding of the sample. At low frequency this shielding corresponds to the Meissner state of the separated filaments in the tape. As the frequency increases, the shielding is achieved first in the whole filamentary zone and then, at higher frequency, in the whole tape.

From the measurements at 7 Hz, the value of χ_0 for the sample **A** is 8.9, while it is 8.8 for the sample **B**. This is not surprising if we consider the very similar geometry of the two tapes.

The comparison between the theoretical and mea-

χ_0	
strip $w_z \times t_z$ Eq. (13)	9.8
strip $w \times t$ Eq. (13)	10.37
x-z array Eq. (14)	9.0
Measured value sample A	8.9
Measured value sample B	8.8

TABLE III: Theoretical and measured χ_0 .

sured values of χ_0 reported in Tab. III shows that the experimental values are close to those theoretically calculated for an x-z array. Looking at the Fig. 4, the χ_0 value is 9.0 at low frequency, it increases up to 9.9 at 510 Hz, and becomes 10.37 at 710 Hz. By comparing these values with the theoretical values reported in Tab. III, we can observe that the value measured at 510 Hz is closer to the one calculated for a infinite strip with rectangular cross section, by taking the width and thickness of the superconducting zone. Furthermore, the value measured at 710 Hz is closer to that calculated for a strip with the

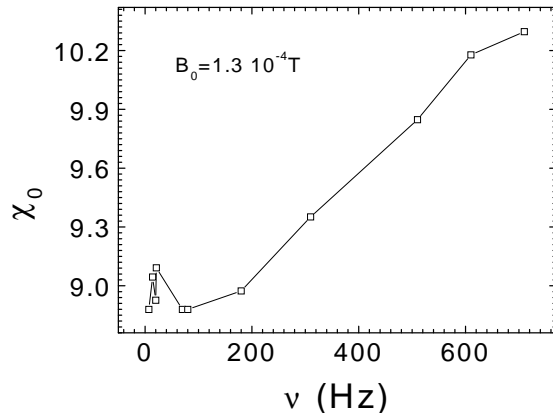


FIG. 4: Frequency dependence of χ_0 as measured on the sample **A** at 1.3 G

whole tape dimensions. Therefore the behaviour of the experimental χ_0 , suggest that the whole tape dimensions can be considered only at higher frequencies.

The interpretation is straightforward: as the frequency increases, a larger volume of the tape is shielded by the current flowing in the metallic matrix, both in the superconducting core and in the central metallic core. Therefore, as the frequency increases, the effective geometry of the sample changes from an x-z array geometry to a monofilamentary strip and therefore, the χ_0 values measured changes accordingly.

B. A.C. susceptibility measurements

In Fig. 5 and in Fig. 6, the real (χ') and the imaginary (χ'') part of the a.c. susceptibility as function of B_0 are shown as measured on the 61.7 mm long sample **A** at different frequencies. In Fig. 5, we can observe that

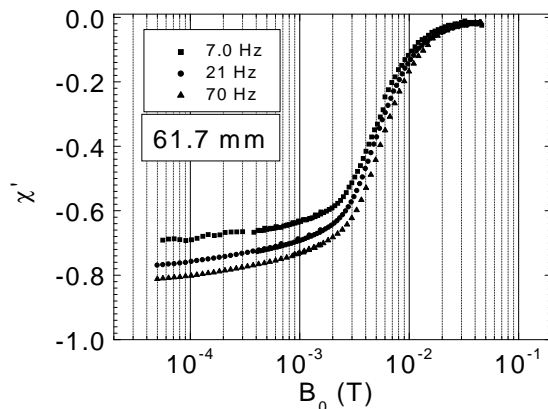


FIG. 5: χ' as function of the magnetic field amplitude B_0 , measured at different frequencies on the 61.7 mm long sample **A**

a larger part of the tape is screened as the frequency of the magnetic field increases. Such frequency dependence has not been observed when χ_0 was determined on much shorter samples. Now, the coupling currents contribute to the overall shielding and thus to χ' . Nevertheless, the correctness of experimental technique is tested by checking that the value of χ' approaches -1 at low field and rises up to 0 at high field.

In Fig. 6 a set of $\chi''(B_0)$ curves, measured in the frequency range from 1 Hz up to 70 Hz, is shown. For frequencies ranging from 1 Hz to 6 Hz our power supply does not allow to reach magnetic fields higher than 1.5 mT. We can observe that χ'' strongly depends on the

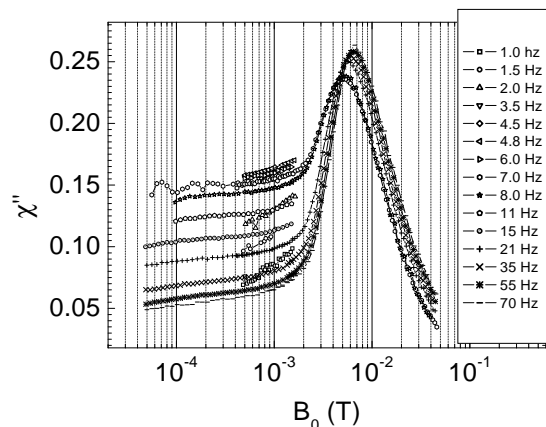


FIG. 6: Measurements of $\chi''(B)$ in the frequency range from 1 Hz to 70 Hz on the 61.7 mm long sample **A**. The curves measured in the 1 Hz - 6 Hz range halt in 1.5 mT

frequency. In the low field region ($B_0 \leq 1$ mT) χ'' depends slightly on B_0 and if we analyze the its frequency behaviour, at fixed B_0 , we find that χ'' reaches its maximum value around 4.8 Hz. However this maximum value is equal to about 0.15 whereas the Campbell model predicts a value of 0.5 (see Eq. (3)). For these reason ,the γ factor introduced in Eq. (3) is equal to 3.3. In the low field region, the light dependence on B_0 and the large frequency dependence are in agreement with the expected behaviour in presence of coupling losses dominant in comparison with the filaments hysteretic losses.

In the high field region, the full coupling among filaments is expected, leading to a behaviour similar to a critical state with the typical peak of χ'' in the amplitude dependence. In this region, as the frequency rises, the maximum value (χ''_{max}) increases and shifts at higher field amplitudes. Such increasing is due to a larger contribution of resistive effects with respect to the critical state²¹. In order to compare the experimental curves with the analytical results for the a.c. susceptibility, the data reported in Fig. 6 have been plotted in Fig. 7 in terms of normalized units χ''/χ''_{max} and $B_0/B_{0,max}$ (where $B_{0,max}$ is the magnetic field amplitude where χ'' has its maximum value). In the same figure, the dotted, dashed and continuous lines are the a.c. suscepti-

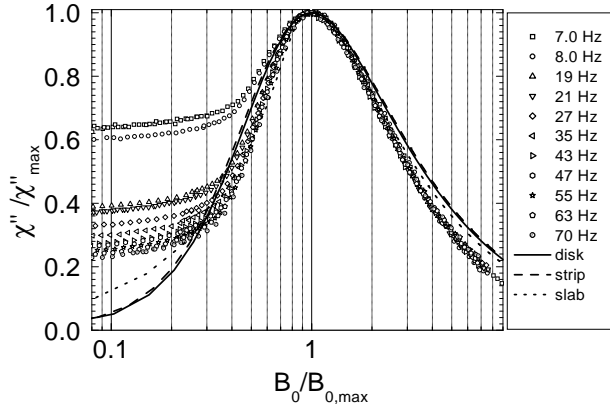


FIG. 7: Measurements of $\chi''(B)$ in the frequency range from 7 Hz to 70 Hz on the sample **A** with length 61.7 mm, plotted in normalized units and compared with the analytical results for different geometries.

bility as calculated in the framework of the critical state model, respectively for a slab^{22,23}, a thin strip²⁴ and a thin disk²⁵. In the high field range, in particular above $B_{0,max}$, the experimental measurements fall on a single curve. The used analytical models do not fit very well the experimental data. However the scaling of the data shows that the sample behaviour, at least in the high field range, can be treated in good approximation within the critical state model framework. Numerical calculations of a.c. susceptibility of a superconducting thick strip^{26,27} could give a better agreement, also taking into account the field dependence of the critical current density ($J(B)$)²⁸ and thermal activated creep phenomena²¹.

V. DISCUSSION

In this section the total losses are determined by using the equation (4) and discussed in the subsection V A. In the subsection V B the losses are analyzed as function of the frequency, at fixed magnetic field amplitudes much lower than the full penetration field of the composite specimen, in order to be in the limit for the validity of the Campbell model. Finally in the last section the effective resistivities are determined and discussed.

A. Total losses

According to equation (3), in Fig. 8 the total losses densities (Q) measured in the sample **A**, 61.7 mm long are reported as function of B_0 , for different frequencies. Very similar dependencies were found for the sample **B**. In Fig. 8 we also report the theoretical slopes expected for the coupling losses in the low field (dotted line) and in the high field (dashed line) regimes. In fact, according to Eq. (2) for B_0 much lower than $B_{0,max}$ the coupling

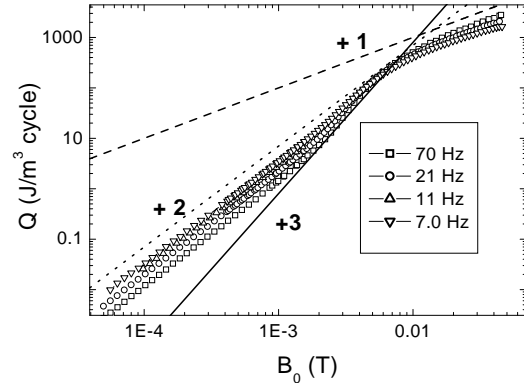


FIG. 8: Total losses density as function of the applied magnetic field, measured on the sample **A** of 61.7 mm long. The dashed and dotted lines are used to compare the experimental data with the expected theoretical slopes for the coupling losses respectively in the low and the high field regions. The continuous line is the theoretical slope as expected for hysteretic losses at fields lower than the full penetration field.

losses should have a quadratic dependence on B_0 . At higher fields, in a critical state description, a cubic dependence can be expected for $B_0 < B_{0,max}$, whereas in the high field region $B_0 > B_{0,max}$ the dependence is linear. Nevertheless for $B_0 \ll B_{0,max}$, a contribution due to the hysteretic losses in the single filaments ($Q_h \propto B_0^3$) should be added to the coupling losses. Therefore in this field region $Q \propto k_1 \times B_0^3 + k_2 \times B_0^2$ where k_1 and k_2 are two proportionality constants and in a log-log plot the slope of the loss density can range from 2 to 3. Our experimental data for fields lower than 1 mT, show a slope very close to the expected value for a pure coupling regime. Deviations from the square slope are observed as the length of the samples is reduced. This is in agreement with the reduction of the coupling loss density as the sample length is reduced, whereas the hysteretic loss density does not change.

B. Frequency dependence of the losses at low magnetic fields

Losses have been investigated as function of the frequency at field much lower than $B_{0,max}$, by measuring several pieces with different lengths, cut from our original samples **A** and **B**. As reported in Fig. 9, the losses exhibit a maximum that shifts towards higher frequencies as the samples length decreases. The experimental data are compared with the results derived from the Campbell model¹³. In particular, the data have been fitted by adding to the coupling loss a frequency independent contribution (β) due to the filaments hysteretic loss:

$$Q_{fit}(\omega) = \alpha \frac{\omega\tau}{1 + \omega^2\tau^2} + \beta \quad (21)$$

For each fit we have used three different parameters, which were not free. In fact, for β we have employed the same value in the three different fits, performed for the samples with different lengths. These values are respectively equal to $\beta=0.29 \text{ J/m}^3 \text{ cycle}$ for the samples **A** and $\beta=0.215 \text{ J/m}^3 \text{ cycle}$ for the samples **B**. Since the hysteretic losses are proportional to the J_c , we compared the ratio $(J_{c,B}/J_{c,A})$, with the ratio of the β values found by the fit. $J_{c,B}/J_{c,A} = 0.743$, that is in good agreement with the ratio $\beta_B/\beta_A = 0.741$.

The parameter α is determined by the maximum value of Q which is equal to $\alpha/2 + \beta$. The α values are in the range $(1.52 \div 1.58) \text{ J/m}^3 \text{ cycle}$ for the sample **A** and in the range $(1.13 \div 1.23) \text{ J/m}^3$ for the sample **B**.

The τ values, obtained from the fits, are reported in Tab. IV whereas in the inset of Fig. 10 its linear dependence on the square of the sample length is shown. The linear fit is very satisfactory for both samples. As shown

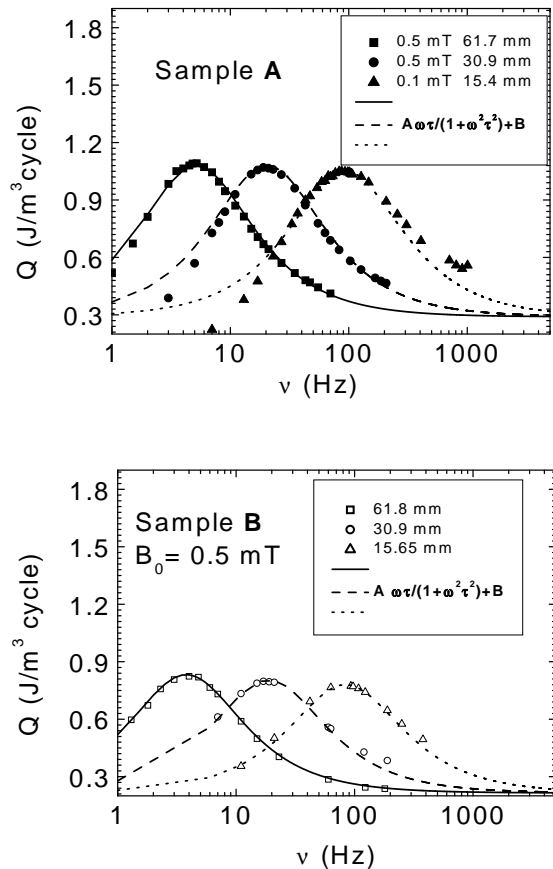


FIG. 9: Frequency dependence of the losses for the sample **A** and the sample **B**, cut in pieces with different lengths. The lines are the fit obtained with the help of the Eq.(20).

in Fig. 9, the fits for the samples **B** are better than those for the samples **A**. The largest deviations are observable for the sample **A** of 15.4 mm length. In fact, for this sample, in Fig. 9 we show the measured losses for a field amplitude of 0.1 mT, because at 0.5 mT the observed

discrepancy between the fit and the experimental data is even larger. This can be ascribed to some other frequency effect which becomes important in the frequency range (100 - 1000 Hz) for pure Ag matrix sample. Indeed,

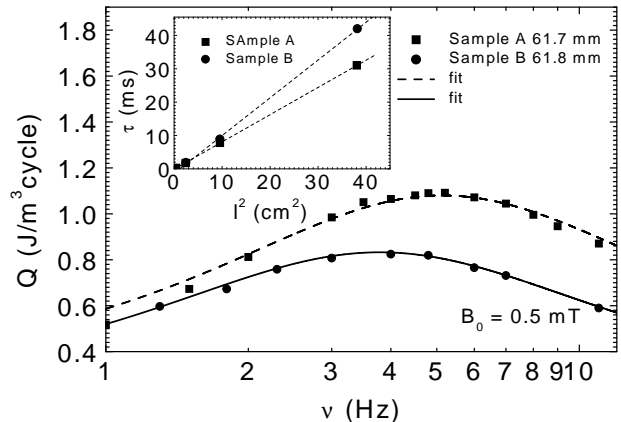


FIG. 10: Comparison between the frequency dependencies of the losses for the samples **A** and **B**, in the frequency region around their maximum. Inset: Dependence of the time constant τ on the square of the sample length (see also Tab. IV.)

As pointed out by Takács^{29,30}, the introduction of two different time constants, τ_0 and τ_1 , in the expression for the coupling losses (see formula (2)) is necessary in the case of flat composite cables, leading to:

$$Q_c = \frac{\gamma B_0^2}{2\mu_0} \left[2\pi\chi_0 \left(\frac{\omega\tau_0}{1 + \omega^2\tau_1^2} \right) \right] \quad (22)$$

In Eq. (22) τ_0 is related to the resistivity of the coupling currents loops and it is determined by the zero frequency limit of $Q(\nu)$, while τ_1 is related to the mean inductance of these loops, and it is determined by the position of the maximum in $Q(\nu)$. Unfortunately, for most of the samples, at low frequencies there are not enough data to be linearly fitted in order to determine the value of τ_0 . Nevertheless, for the 15.5 mm long sample **A** this fitting procedure has been possible, and the value for τ_0 has been estimated to be 1.5 ms, which is not so different from 1.7 ms found for τ_1 by using the same data. Increasing the length of the sample, the frequency where the maximum in $Q(\nu)$ occurs decreases and therefore a smaller difference between τ_0 and τ_1 is expected.

C. Effective Resistivity

By using the experimental values of τ and χ_0 , the effective resistivity of the metallic matrix has been determined.

For samples with the same length and the same geometry the relation $\tau_A/\tau_B = \rho_B/\rho_A$ is valid. If $\rho_A < \rho_B$ we should have $\tau_A > \tau_B$, which means that the frequency (ν_{max}) where the maximum in the $Q_c(\nu)$ occurs

ℓ (mm)	τ (ms)	χ_0	ρ_{eff} ($\mu\Omega$ cm)
sample A			
61.7	31	8.9	0.176
30.9	7.8	8.9	0.175
15.5	1.75		0.192
6.5	0.32	9.8	0.172
sample B			
61.8	42	8.8	0.132
30.9	8.9	8.8	0.155
15.6	1.9	9.0	0.182

TABLE IV: Values of the quantities τ , χ_0 and ρ_{eff} as determined from the experimental data for all the considered samples.

is lower for the sample with lower resistivity. The directly measured matrix resistivity of the sample **A** is 4 times smaller than that for the sample **B** (see section III A). Since the structure of the samples is very similar (as confirmed by the experimentally found values of χ_0), we expect ($\nu_{max,A} < \nu_{max,B}$). It is striking to see that the experimental data in Fig. 10 demonstrate the opposite behaviour. The obtained results are summarized in Tab. IV. For the sample **A**, the value of the effective resistivity is 3 times higher than the value expected from Eq. (11). Moreover the effective resistivity found for the sample **B** is lower than both the ρ_{eff} of the sample **A**, and its ρ_{eff} determined by Eq. (11). This can be understood if the structure of the sample is considered. In Fig. 11 the micrographs of a section of both the samples **A** and **B** are shown. In the sample **B** many intergrowths in the metallic matrix are visible. Intergrowths between columns can generate paths with lower resistivity for the flowing of the coupling currents. The presence of intergrowths reduces or cancels the advantage coming from the use of a matrix with higher resistivity in order to decrease the coupling losses.

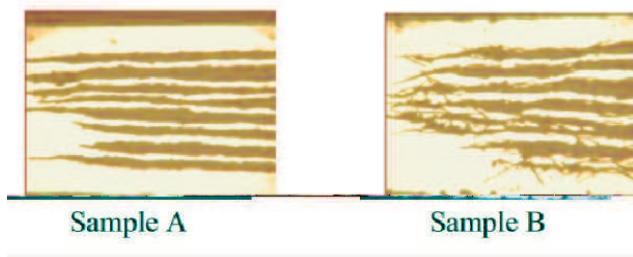


FIG. 11: Micro-graphs of a cross section of the sample **A** and **B**. In the sample **B** the intergrowths are clearly visible.

On the contrary, the sample **A** shows a value of ρ_{eff} which is higher than the expected one. This high value

can be due to a contact resistance between the superconducting filaments and the metallic matrix.

VI. CONCLUSIONS

In this work we have studied the a.c. coupling losses on two different sets of bicolumnar BSCCO tapes.

For the geometrical factor χ_0 , we used the experimental value instead of the demagnetizing factor ($t_z + w_z/t_z$) used in literature^{7,9,10} which should give the found value 13.5 instead of the value 8.9, for both samples. Our experimental value is in agreement with the theoretical value computed for an x-z finite array. In this way the main physical quantity involved in the coupling losses have been experimentally estimated.

For increasing frequencies the measured χ_0 approaches the value calculated for a superconducting strip with the width and the thickness equal to the dimensions of the elementary zone of the tape. By further frequency increasing, χ_0 approaches the value calculated for a superconducting strip with dimensions equal to those of the full tapes.

A.C. susceptibility and losses, measured as function of the magnetic field amplitude and frequency, confirm that the coupling losses dominate in these samples over the hysteretic losses of the single filaments. The frequency dependence of the experimentally measured losses at low field has been analyzed by using the Campbell model and a good agreement between the model and the experimental data has been obtained. The time constants τ of the tape has been determined for different lengths of the sample, finding, as expected, a linear dependence of τ on the square of the sample length. The final task has been the experimental evaluation of the effective resistivity. In the sample **A** with a pure silver matrix, the high value measured for ρ_{eff} is interpreted as bad electrical contacts between the filaments and the metallic matrix. In the sample **B**, the experimentally found value ρ_{eff} lower than the expected one in an ideal sample, is explained with the presence of intergrowths. This particular result suggests that in this kind of samples, the enhancement of the effective matrix resistivity does not reduce intrinsically the coupling losses.

Finally it is worth to point out that for low magnetic field amplitudes, the Campbell model can be successfully used also for BSCCO tapes containing few flat filaments. This can be used as a starting point to analyze all the other factors which influence the losses in more complex geometries.

VII. ACKNOWLEDGEMENTS

We thank Jano Šouc for helpful discussion and Juraj Tancar for his technical support.

* Corresponding author;
e-mail: zoldan@sa.infn.it;

- ¹ S. Takács, *Superconducting Science and Technology* **10**, 733 (1997).
- ² J. Clem, *AC Losses in Type II superconductors* (in *Magnetic Susceptibilities of Superconductors and Other Systems* Edited by A. Hein et al., 1991).
- ³ K. Kwasnitza, *Cryogenics* **17**, 617 (1977).
- ⁴ K. Kwasnitza and S. Clerc, *Physica C* **233**, 423 (1994).
- ⁵ M. Oomen, J. Rieger, M. Leghissa, and H. ten Kate, *Physica C* **290**, 281 (1997).
- ⁶ K. Kwasnitza, S. Clerc, R. Flükiger, and Y. Huang, *Physica C* **299**, 113 (1998).
- ⁷ K. Kwasnitza, S. Clerc, R. Flükiger, and Y. Huang, *Cryogenics* **39**, 829 (1999).
- ⁸ M. D. Sumption, E. Lee, and E. W. Collings, *Physica C* **337**, 187 (2000).
- ⁹ K. Kwasnitza, S. Clerc, R. Flükiger, G. Witz, and Y. Huang, *Physica C* **355**, 325 (2001).
- ¹⁰ H. Eckelmann, L. Krempasky, and C. Schmidt, *Physica C* **370**, 177 (2002).
- ¹¹ P. Fabbriatore, S. Farinon, S. Innocenti, and F. Gömör, *Physical Review B* **61**, 6413 (2000).
- ¹² P. Fabbriatore, S. Farinon, F. Gömör, and S. Innocenti, *Superconducting Science and Technology* **13**, 1327 (2000).
- ¹³ A. M. Campbell, *Cryogenics* **22**, 3 (1982).
- ¹⁴ G. Ries, *IEEE Transaction Magnetics* **13**, 524 (1977).
- ¹⁵ D. Zola, M. Polichetti, C. Senatore, T. D. Matteo, and S. Pace, unpublished (2003).
- ¹⁶ M. D. Sumption, E. Lee, S. X. Dou, and E. W. Collings, *Physica C* **335**, 164 (2000).
- ¹⁷ D. Zola, M. Polichetti, C. Senatore, T. D. Matteo, and S. Pace, *Physica C* **372-376**, 1823 (2002).
- ¹⁸ W. Carr, *AC Loss and macroscopic theory of superconductors* (New York: Gordon and Breach, 1983).
- ¹⁹ M. Oomen, J. Rieger, M. Leghissa, and B. ten Haken, *Superconducting Science and Technology* **13**, 1101 (2000).
- ²⁰ Y. Mawatary, *Physical Review B* **54**, 13215 (1996).
- ²¹ D. D. Gioacchino, F. Celani, P. Tripodi, A. M. Testa, and S. Pace, *Physical Review B* **60**, 13112 (1999).
- ²² C. Bean, *Physical Review Letter* **8**, 250 (1962).
- ²³ R. B. Goldfarb, M. Leental, and C. A. Thompson (in *Magnetic Susceptibilities of Superconductors and Other Systems* Edited by A. Hein et al., 1991).
- ²⁴ E. H. Brandt, *Physical Review B* **49**, 9024 (1994).
- ²⁵ J. R. Clem and A. Sanchez, *Physical Review B* **50**, 9355 (1994).
- ²⁶ E. H. Brandt, *Physical Review B* **54**, 4246 (1996).
- ²⁷ E. H. Brandt, *Physical Review B* **58**, 6523 (1998).
- ²⁸ F. S. a, F. Gömör, R. Tebano, and E. Seiler, *Physica C* **372-376**, 977 (2002).
- ²⁹ S. Takács, *Physica C* **354**, 202 (2001).
- ³⁰ S. Takács and J. Yamamoto, *Time constants of flat superconducting cables*, vol. 42 of *Advances in Cryogenics Engineering* (Edited L.T. Summers, 1996).